*Journal of Sound and Vibration* (2001) **239**(1), 41–56
doi:10.1006/jsvi.2000.3155, available online at http://www.idealibrary.com on IDEAL®

# A GLOBAL SMOOTHING TECHNIQUE FOR FRF DATA FITTING

R. RUOTOLO

*Department of Aeronautical and Space Engineering, Politecnico di Torino, corso Duca degli Abruzzi* 24, *Torino, Italy. E-mail: ruotolo@athena.polito.it*

AND

D. M. STORER

*Centro Ricerche FIAT, Strada Torino*, 50, *Orbassano, Italy*

(*Received* 26 *October* 1999, *and in final form* 22 *May* 2000)

In previous studies, the method originally proposed by Dat and Meurzec for curve-fitting a modal model to frequency response functions has been demonstrated to be an extremely interesting means of analyzing data measured from structures which exhibit close modes and/or high level of damping i.e., high modal coupling. The aim of the research described in this article was to develop this technique in order to deal with multi-input multi-output systems, usually encountered in vibration testing, and to improve the numerical conditioning of the method by introducing orthogonal polynomials. Two practical applications using experimental data measured during vibration tests on cars are described in order to demonstrate the properties of this improved version and, when appropriate, occasional comparisons with other more conventional curve-fitting techniques are included.


## 1. INTRODUCTION

The significant advances in measurement instrumentation seen in recent years have helped contribute to the increase in experimental testing of structural systems in both academic research laboratories and in industry. Experimental tests to characterize the dynamic behaviour of structures and components are commonly required during the design and development phase of a product, and increasingly in-service monitoring during its lifetime is also being requested. Often the aim is to use the accurate information obtained during characterization tests to predict the dynamic behaviour of the system in specific operating conditions.

In the field of structural dynamics in mechanical systems, widespread use is made of modal testing, an experimental technique for evaluating the modal properties (natural frequencies and mode shapes) based on the assumption that the dynamic behaviour of the structure under test is nominally linear. By using a range of curve-fitting techniques available in commercial software packages, the measured frequency response functions (FRFs) can be processed in order to obtain a reduced order, mathematical modal model that represents the dynamic characteristics of the structure over the finite bandwidth of the test data.

Although several alternatives for curve-fitting measured FRFs are often available to the experimental analyst, in practice each of the commonly available techniques, irrespective of

0022-460X/01/010041 + 16 $35.00/0 

whether the estimation process uses data in the time or frequency domain, suffers drawbacks when the structure exhibits a high degree of modal coupling, i.e., in the presence of high damping and close modes.

In general, it has been demonstrated that frequency domain methods tend to perform better than time domain methods in estimating modal properties of systems with high modal coupling [1] since the broad resonance peaks in the FRFs, characteristic of highly damped structures, correspond to impulse response functions with effectively short duration in time. (A survey of the various multivariable frequency domain estimators is given in reference [2].)

One of the most challenging applications for modal curve-fitting is the analysis of data acquired during aircraft flight flutter test sessions since the measured signals are generally subject to high noise levels and the aircraft structure usually has high modal coupling. For these reasons the Dat and Meurzec smoothing technique [3], a technique developed for this application and employed successfully by Italian aeronautical companies [4, 5], was considered to be particularly interesting for extension to other structural systems.

In references [6, 7] the rational fraction polynomial (RFP) [8] method, based on the least-squares method (LSM) and analyzing frequency domain data, was shown to yield imprecise results for noisy data and/or high modal coupling. The LSM does not lead to the minimization of the true error particularly in the region of the natural frequencies; in general, the error tends to be higher at low frequencies and lower at high frequencies, the so-called localization and imbalance effects. This is the main reason why a poor fit is obtained when LSM-based system identification techniques are applied. After analyzing the reasons for biased estimates, an improved version of RFP (called IRFP) was formulated which leads to the minimization of the true fitting error by using a non-linear procedure [6].

Through the research which is documented in this article, it was demonstrated that the smoothing technique minimizes the true error fitting. At the outset of the project it was found that, as formulated by Dat and Meurzec, the original smoothing technique was applicable only for single-input single-output (SISO) systems [3]. However, in order to obtain a more complete description of the dynamic characteristics of the structure under test, it is usual to use many measurement transducers (e.g., accelerometers) distributed over the structure in order to permit interpretation of the resulting mode shapes and apply excitation at more than one point and in more than one direction; as a consequence, the need arises for techniques that can analyze multi-input multi-output (MIMO) systems.

Preliminary results on the extension of the smoothing technique have been presented previously [5, 9]; initially, the original method proposed by Dat and Meurzec was extended to deal with MIMO systems, even though currently it is only possible to provide an estimation of the poles from the MIMO FRFs [5]. The aspect of the robustness of the method for analyzing data with high damping was addressed subsequently [9]. Nevertheless, the first implementation of this method suffered from numerical conditioning problems during matrix inversions, and subsequently it has been discovered that this problem can be avoided by using routines in Matlab [10], although when large data sets need to be analyzed, as results for example from tests on a car, this does not represent a feasible solution and the aspect of numerical conditioning remains pertinent.

This paper describes recent developments made to improve and extend the original smoothing technique: different ways for solving the numerical conditioning problems arising from the high order polynomials can be considered [11], resulting in the selection of Forsythe's orthogonal polynomials [12], which were originally used for system identification in the orthogonal polynomial method proposed by Van der Auweraer and Leuridan [13]. To demonstrate the robustness of this new method, called global smoothing

technique in this work, with respect to high modal coupling, two examples related to automotive engineering complete the article.

## 2. FORMULATION OF THE TECHNIQUE WITH ORTHOGONAL POLYNOMIALS

### 2.1. BASIS OF THE METHOD

By using a common denominator parametrization [2], it is possible to formulate an expression for each FRF of a set of $M = N_i \times N_o$ Frequency Response Functions under analysis (where $N_i$ is the number of inputs and $N_o$ is the number of outputs present during the test), namely

$$H^{(i)}(s) = \frac{\sum_{r=0}^{n_a} a_r^{(i)} p_r(s)}{\sum_{r=0}^{n_b} b_r q_r(s)} = \frac{P^{(i)}(s)}{Q(s)}, \tag{1}$$

in which $p_r(s)$ and $q_r(s)$ are polynomials and $s = \mathrm{j}\omega$. This expression illustrates that the denominator is the same for all FRFs, with the meaning that all FRFs are characterized by the same poles (the roots of the denominator) because they are global quantities. Moreover, the orders of numerator and denominator, $n_a$ and $n_b$, respectively, are related according to the expression

$$n_a = n_b - g, \tag{2}$$

where $g$ has different values according to the type of measured FRF: $g = 2$ for receptance, $g = 1$ for mobility and $g = 0$ for inertance. (In some cases $g$ can assume even negative values in order to compensate for out-of-band modes.) In addition, $n_b$ is equal to double the number of modes present in the frequency band under analysis [14].

If $H_m^{(i)}$ denotes the FRF to be curve-fitted, the error resulting from the approximation is given by

$$e_T^{(i)}(s) = H^{(i)}(s) - H_m^{(i)}(s) = \frac{P^{(i)}(s)}{Q(s)} - H_m^{(i)}(s). \tag{3}$$

Multiplying both sides of equation (3) by $Q(s)D(s)$, where $D(s)$ is a weighting function to be selected following the criteria to be described subsequently, one obtains

$$D(s)Q(s)e_T^{(i)}(s) = D(s)P^{(i)}(s) - D(s)Q(s)H_m^{(i)}(s). \tag{4}$$

The left-hand side of expression (4) is the error which is minimized by applying the procedure originally proposed by Dat and Meurzec [3]; expression (4) can be rewritten as

$$e^{(i)}(s) = D(s)P^{(i)}(s) - D(s)Q(s)H_m^{(i)}(s). \tag{5}$$

Accordingly, it is possible to introduce an error function given by

$$J^{(i)}(s) = e^{(i)*}(s)e^{(i)}(s), \tag{6}$$

so that minimizing the error over a given bandwidth $I_\omega$ corresponds to determining the minimum of

$$\int_{\mathrm{j}I_\omega} J^{(i)}(s)\,\mathrm{d}s \approx \Delta s \sum_{k \in I_k} J^{(i)}(s_k),$$

upon remembering that all FRFs have been measured at discrete values of the independent variable: $s_k = j\omega_k$ with $k \in 1, \ldots, n_k = I_k$. Moreover, $\Delta s = s_{k+1} - s_k$.

As previously stated, the error given by equation (5) can be computed when the weighting function $D(s)$ is known. Dat and Meurzec [3] proposed the weighting function

$$D(s) = |Q(s)|^{-1}, \tag{7}$$

justifying the selection on the grounds that "close to the poles, where $Q(s)$ is very low, the function $D(s)$ must assume a high value such that the term $D(s)Q(s)H_m^{(i)}(s)$ has the same magnitude in all the bandwidth".

According to equations (4) and (5), it is clear that by using the former expression for $D(s)$ the error minimized by the original smoothing technique is

$$e^{(i)}(s) = D(s)Q(s)e_T^{(i)}(s) = \frac{Q(s)}{|Q(s)|}\, e_T^{(i)}(s),$$

and, as a result, the error function has the expression

$$J^{(i)}(s) = e^{(i)*}(s)e^{(i)}(s) = \frac{Q^*(s)Q(s)}{|Q(s)|^2}\, e_T^{(i)*}(s)e_T^{(i)}(s) = e_T^{(i)*}(s)e_T^{(i)}(s). \tag{8}$$

Expression (8) highlights the most important property of this technique: by selecting $D(s) = |Q(s)|^{-1}$, the true error can be minimized resulting in a curve-fitted function which approximates closely to the measured FRFs even if the system under test is characterized by high modal coupling. In section 3, this property is demonstrated by using experimental results.

### 2.2. USE OF MATRIX FORMULATION

As stated in equation (1), the polynomials $P^{(i)}(s)$ and $Q(s)$ depend on the coefficients $a_r^{(i)}$ and $b_r$. Consequently, in order to use a matrix formulation, the following magnitudes can be introduced:

$$u_{k,r} = D(s_k)p_r(s_k), \quad v_{k,r}^{(i)} = D(s_k)q_r(s_k)H_m^{(i)}(s_k). \tag{9}$$

These represent the elements of matrices $[U]$ and $[V^{(i)}]$ respectively.

By introducing these magnitudes into equation (5), and evaluating the error $e^{(i)}(s)$ at each measurement frequency $\omega_k$, the resulting quantities can be incorporated into a vector $\{e^{(i)}\}$ to yield the expression

$$\{e^{(i)}\} = [U]\{a^{(i)}\} - [V^{(i)}]\{b\} = [[U] - [V^{(i)}]] \begin{Bmatrix} \{a^{(i)}\} \\ \{b\} \end{Bmatrix}, \tag{10}$$

where all coefficients $a_r^{(i)}$ and $b_r$ are contained in vectors $\{a^{(i)}\}$ and $\{b\}$ respectively. Equation (10) can be rewritten as

$$\{e^{(i)}\} = [[U] - [V^{(i)}]]\,\{\theta^{(i)}\} \tag{11}$$

with

$$\{\theta^{(i)}\} = \begin{Bmatrix} \{a^{(i)}\} \\ \{b\} \end{Bmatrix}.$$

In order to reduce the approximation error, the error function defined in equation (6) can be used by calculating the summation value across the bandwidth of interest:

$$J^{(i)}(\{\theta^{(i)}\}) = \{e^{(i)}\}^{\mathrm{H}}\{e^{(i)}\}. \tag{12}$$

Here the superscript H denotes the complex conjugate transposition. By introducing expression (11) into equation (12), the error function can be expressed as

$$J^{(i)}(\{\theta^{(i)}\}) = \{\theta^{(i)}\}^{\mathrm{T}}\begin{bmatrix} [L_1] & -[L_{1i}] \\ -[L_{1i}]^{\mathrm{H}} & [L_{ti}] \end{bmatrix}\{\theta^{(i)}\} \tag{13}$$

with

$$[L_1] = [U]^{\mathrm{H}}[U], \quad [L_{1i}] = [U]^{\mathrm{H}}[V^{(i)}], \quad [L_{ti}] = [V^{(i)}]^{\mathrm{H}}[V^{(i)}]. \tag{14}$$

The error function $J^{(i)}(\{\theta^{(i)}\})$ can be evaluated for each measured FRF; the simplest way to take into account all the measured FRFs is to introduce a total error $J(\{\Theta\})$ defined as the sum of all error functions $J^{(i)}(\{\theta^{(i)}\})$:

$$J(\{\Theta\}) = \sum_{i=1}^{M} J^{(i)}(\{\theta^{(i)}\}). \tag{15}$$

By collecting all the coefficients $a_r^{(i)}$ and $b_r$ to be estimated into the vector $\{\Theta\}$,

$$\{\Theta\} = \begin{Bmatrix} \{a^{(1)}\} \\ \{a^{(2)}\} \\ \vdots \\ \{a^{(M)}\} \\ \{b\} \end{Bmatrix}, \tag{16}$$

the total error can be easily rewritten as

$$J(\{\Theta\}) = \{\Theta\}^{\mathrm{T}}[\Lambda]\{\Theta\}, \tag{17}$$

with

$$[\Lambda] = \begin{bmatrix} [L_1] & [0] & [0] & \cdots & -[L_{11}] \\ [0] & [L_1] & [0] & \cdots & -[L_{12}] \\ [0] & [0] & [L_1] & \cdots & -[L_{13}] \\ \vdots & \vdots & \vdots & \ddots & \vdots \\ -[L_{11}]^{\mathrm{H}} & -[L_{12}]^{\mathrm{H}} & -[L_{13}]^{\mathrm{H}} & \cdots & [L_t] \end{bmatrix},$$

where

$$[L_t] = \sum_{i=1}^{M} [L_{ti}]. \tag{18}$$

### 2.3. USE OF ORTHOGONAL POLYNOMIALS

In references [5, 9] it was demonstrated that the extension of the original smoothing technique to MIMO systems involves the inversion of matrices $[L_1]$ and $[L_t]$. In certain

situations, this inversion is ill-conditioned giving rise to imprecise estimates for the coefficients $a_r^{(i)}$ and $b_r$ and, as a consequence, to poor-quality FRF curve-fits and inaccurate estimates of the poles. Thus, Forsythe's orthogonal polynomials are proposed for expressing both $p_r(s)$ and $q_r(s)$ [12], such that both $[L_1]$ and $[L_t]$ will be identity matrices. These polynomials have the useful property of orthogonality over the interval $I_s$ with respect to the weighting functions $W_p(s)$ and $W_q(s)$ respectively, which can be expressed as

$$\int_{I_s} p_i^*(s)\, W_p(s) p_j(s)\, \mathrm{d}s = \delta_{ij}, \quad \int_{I_s} q_i^*(s)\, W_q(s) q_j(s)\, \mathrm{d}s = \delta_{ij}, \tag{19}$$

where $\delta_{ij}$ is Kronecker's delta function. When both the interval of calculation $I_s$ and the weighting function $W(s)$ are known, the evaluation of the polynomials can be performed by using the approach described in reference [12].

By using expressions (9) and (14), the generic element for matrix $[L_1]$ can be calculated as

$$[L_1]_{ij} = \sum_{k \in I_k} D^*(s_k) p_i^*(s_k) D(s_k) p_j(s_k), \tag{20}$$

where the superscript * denotes complex conjugation. From the comparison of equation (20) with the first of equations (19) after transforming integrals into summations, it is clear that the weighting function related to polynomial $p_r(s)$ is

$$W_p(s) = D^*(s) D(s) = |D(s)|^2. \tag{21}$$

Similarly, by using expressions (9), (14) and (18), the generic element for matrix $[L_t]$ is given by

$$\begin{aligned}
[L_t]_{ij} &= \sum_{l=1}^{M} ([V^{(l)}]^{\mathrm{H}} [V^{(l)}])_{ij} \\
&= \sum_{k \in I_k} \sum_{l=1}^{M} D^*(s_k) H_m^{(l)*}(s_k) q_i^*(s_k) D(s_k) H_m^{(l)}(s_k) q_j(s_k) \\
&= \sum_{k \in I_k} q_i^*(s_k) \left( |D(s_k)|^2 \sum_{l=1}^{M} |H_m^{(l)}(s_k)|^2 \right) q_j(s_k).
\end{aligned}$$

As a consequence, the weighting function for polynomials $q_r(s)$ is

$$W_q(s) = |D(s_k)|^2 \sum_{l=1}^{M} |H_m^{(l)}(s_k)|^2. \tag{22}$$

It is interesting to observe that even if the aim of this technique is to curve-fit $M$ FRFs, the introduction of orthogonal polynomials requires the evaluation of just two weighting functions which hold for each measured FRF.

As a result of introducing these orthogonal polynomials, the expression for matrix $[\Lambda]$ can be simplified to

$$[\Lambda] = \begin{bmatrix}
[I] & [0] & [0] & \cdots & -[L_{11}] \\
[0] & [I] & [0] & \cdots & -[L_{12}] \\
[0] & [0] & [I] & \cdots & -[L_{13}] \\
\vdots & \vdots & \vdots & \ddots & \vdots \\
-[L_{11}]^{\mathrm{H}} & -[L_{12}]^{\mathrm{H}} & -[L_{13}]^{\mathrm{H}} & \cdots & [I]
\end{bmatrix}, \tag{23}$$

demonstrating that all the matrices along the principal diagonal of matrix $[\Lambda]$ are now transformed into the identity matrix, while all the other matrices $[L_{1i}]$ are defined according to equation (14).

By examining expression (17), it is evident that the minimum value for the total error function $J(\{\Theta\})$ corresponds to a null vector $\{\Theta\}$. Therefore, in order to obtain a non-zero solution, a constraint must be introduced:

$$\gamma(\{\Theta\}) = \{\Theta\}^{\mathrm{T}}[R]\{\Theta\} - 1 = 0, \tag{24}$$

where the value for matrix $[R]$ is specified subsequently.

The minimization of function $J(\{\Theta\})$ constrained by condition (24) can be performed by using Lagrange's multipliers [15], i.e., solving the system of equations

$$\left\{\begin{array}{r} \dfrac{\partial J(\{\Theta\})}{\partial\{\Theta\}} - \lambda\dfrac{\partial\gamma(\{\Theta\})}{\partial\{\Theta\}} = 0, \\ \\ \gamma(\{\Theta\}) = 0. \end{array}\right\}$$

By taking into account equations (17) and (24) the first of these equations becomes

$$[\Lambda]\{\Theta\} - \lambda[R]\{\Theta\} = 0.$$

By multiplying the previous expression by $\{\Theta\}^{\mathrm{T}}$ and using condition (24), it follows that

$$J(\{\Theta\}) = \lambda,$$

so that the following relation holds:

$$[\Lambda]\{\Theta\} - J(\{\Theta\})[R]\{\Theta\} = 0. \tag{25}$$

The next step is to select a particular value for matrix $[R]$,

$$[R] = \begin{bmatrix} [0] & [0] & \cdots & [0] \\ [0] & [0] & \cdots & [0] \\ \vdots & \vdots & \ddots & \vdots \\ [0] & [0] & \cdots & [I] \end{bmatrix},$$

so that when introduced into expression (25) the calculation can be simplified; indeed the first $M$ matrix equations of (25) reduces to

$$\{a^{(i)}\} = [L_{1i}]\{b\}, \tag{26}$$

and this, introduced in the last equation, provides

$$\left(\sum_{i=1}^{M} -[L_{1i}]^{\mathrm{H}}[L_{1i}] + [I](1 - J(\{\Theta\}))\right)\{b\} = 0. \tag{27}$$

By calling

$$1 - J(\{\Theta\}) = \mu$$

equation (27) becomes

$$([G] - \mu[I])\{b\} = 0, \tag{28}$$

with

$$[G] = \sum_{i=1}^{M} [L_{1i}]^{\mathrm{H}} [L_{1i}]. \tag{29}$$

A non-zero solution of equation (28) can be obtained by evaluating the eigenvalues of the matrix $[G]$; the maximum eigenvalue is that one for which the total error $J(\{\Theta\})$ is minimum, such that the corresponding eigenvector provides the estimate for coefficients $b_r$, while all the coefficients $a_r^{(i)}$ can be evaluated through equation (26).

Natural frequencies and corresponding damping ratios can be extracted from the roots of the denominator, i.e., the poles of the analyzed system, by recalling that firstly the polynomial has real coefficients such that it has $n_b/2$ couples of complex conjugate roots $\lambda$, $\lambda^*$. Secondly, every pole $\lambda$ is related to the corresponding natural circular frequency $\omega_n$ and damping ratio $\zeta$ according to

$$\lambda = \omega_n(-\zeta + \mathrm{j}\sqrt{1-\zeta^2}). \tag{30}$$

As a result, the natural circular frequency can be evaluated as

$$\omega_n = |\lambda|,$$

and the damping ratio is given by

$$\zeta = -\frac{\mathrm{real}(\lambda)}{\omega_n}.$$

Clearly, $D(s)$ can be set according to relation (7) only when a first estimate for the denominator $Q(s)$ is available. As a consequence, as mentioned in references [3, 5, 9] it has been suggested to start with an estimate obtained with a rational fraction polynomial for $D(s)$ and continue by introducing into $D(s)$ the last estimate for $|Q(s)|^{-1}$. This iterative procedure concludes when the error in the curve-fitting ceases to decrease.

## 3. APPLICATION TO EXPERIMENTAL DATA

### 3.1. ENGINE VIBRATION TESTING DATA

The aim of this case study is to demonstrate the potential of the global smoothing technique (GST) described in the previous section and illustrate in a comparison that this new technique may offer certain advantages over other more conventional alternatives such as the rational fraction polynomial (RFP) Method (although a detailed comparison analysis is beyond the scope of this study).

The data used in this case study were measured during a stepped-sine test on a normal production vehicle, using a "4-poster" road simulator, exciting the forward left wheel at the tyre patch and in the vertical direction and measuring the vibrational response at different points on the engine. By using the acceleration at the hub of the excited wheel as the reference signal, and measuring the acceleration response on the engine in correspondence with engine mount attachments, it was possible to measure a set of transmissibility functions which represent a useful indicator of the global dynamics of the vehicle in the lower frequency range. (The layout of the excitation point and of measuring locations is illustrated in Figure 1.)

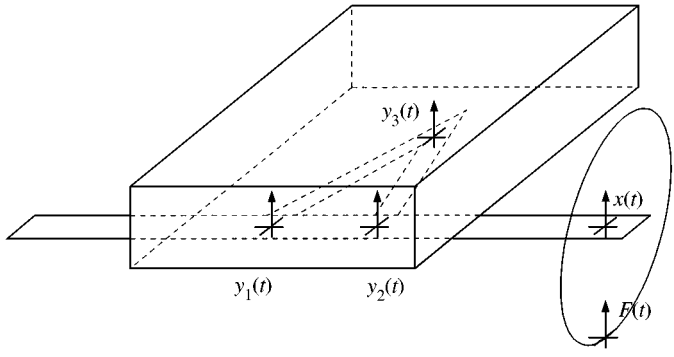


Figure 1. Excitation and measurement points on the engine.

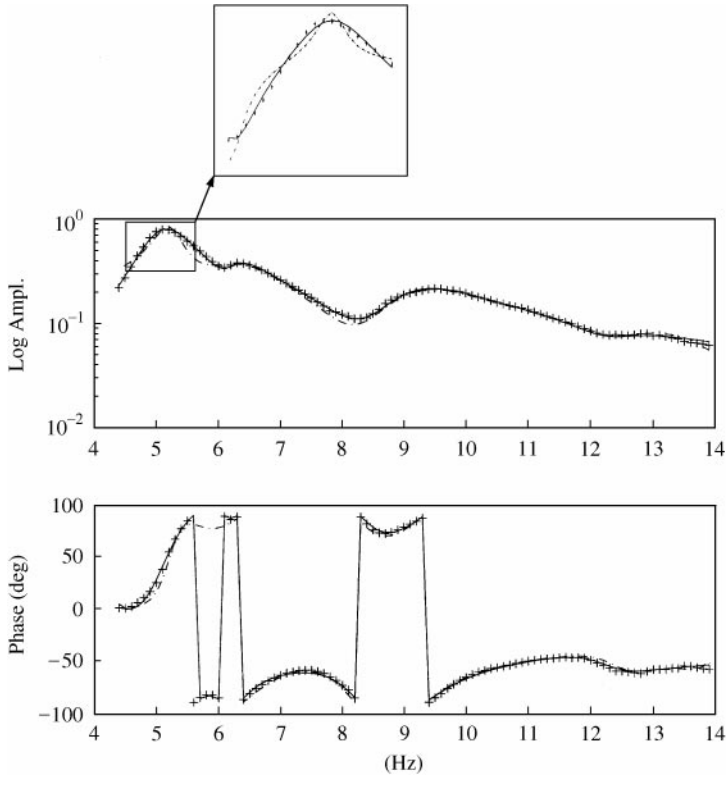


Figure 2. Transmissibility between $y_1(t)$ and $x(t)$ (+: experimental data, — GST, – · – RFP).

Figures 2–4 illustrate results of curve-fitting the transmissibility functions using GST and RFP and Table 1 shows the modal parameters determined by the two methods; the pole estimates for the latter method have been obtained by applying the stabilization diagram procedure. As can be observed, the accuracy of the fitting obtained with GST is better than that of RFP in particular in the region of the resonance at about 5 Hz, mainly due to underestimation of the damping ratio of this mode and overestimation of the damping ratio of the following mode by RFP. Both the methods indicate that four modes are present in the frequency range of interest, although with GST a dominant mode at 3·5 Hz is exhibited which certainly influences the transmissibility curve towards the lower end of the frequency

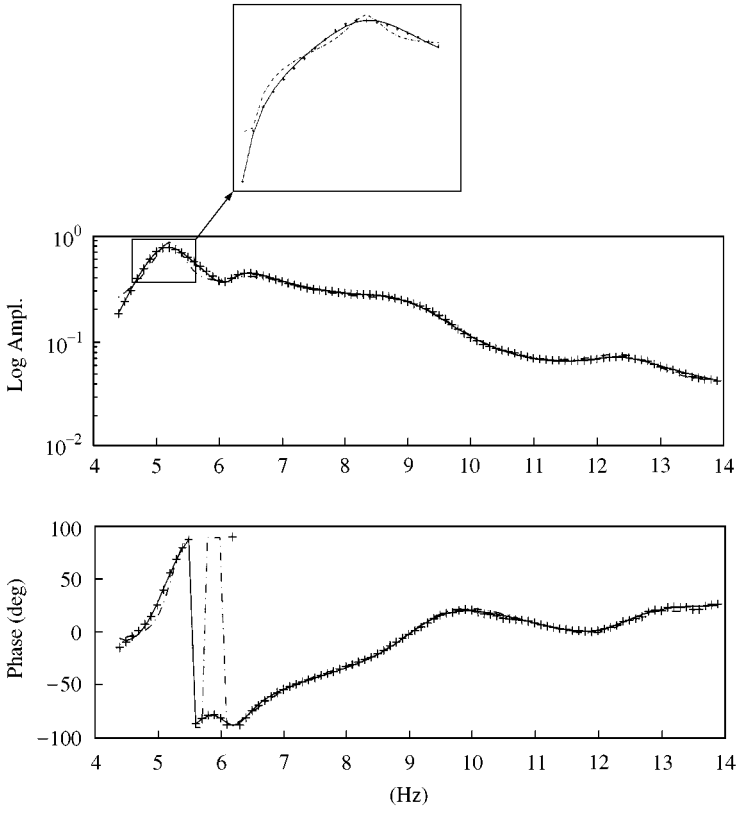


Figure 3. Transmissibility between $y_2(t)$ and $x(t)$ (+: experimental data, — GST, – · – RFP).

interval considered. As can be observed and as occurred by using the IRFP proposed in reference [6], the number of modes necessary to obtain a good curve-fit using the GST is equal to the number of modes effectively present in the frequency band of interest. Therefore it is not necessary to specify a higher number of modes than necessary, in contrast to that which is usually required when applying RPF using the stabilization diagram.

In Figure 5 a comparison between the true error fitting relative to the two techniques is shown. In this figure a cumulative transmissibility is plotted, obtained as the summation of absolute values of the three transmissibilities, to facilitate the identification of the system resonances. In addition, the true error fitting relative to both RFP (dashed line) and GST (dash–dot line) is shown. It is clear that the RFP error is higher close to the dominant system resonances, which is the localization error described in reference [6], and its peak value is higher than the corresponding one of GST. Moreover, the error obtained by applying GST is almost constant over the entire frequency range.

### 3.2. FULL-TRIMMED CAR BODY

The main aim of this second example is to illustrate the effectiveness of GST for curve-fitting FRFs measured from structural systems with high modal coupling.

The FRFs to be analyzed were measured during vibration testing of a full-trimmed car body, which was suspended on elastic cords in order to create nominally free–free

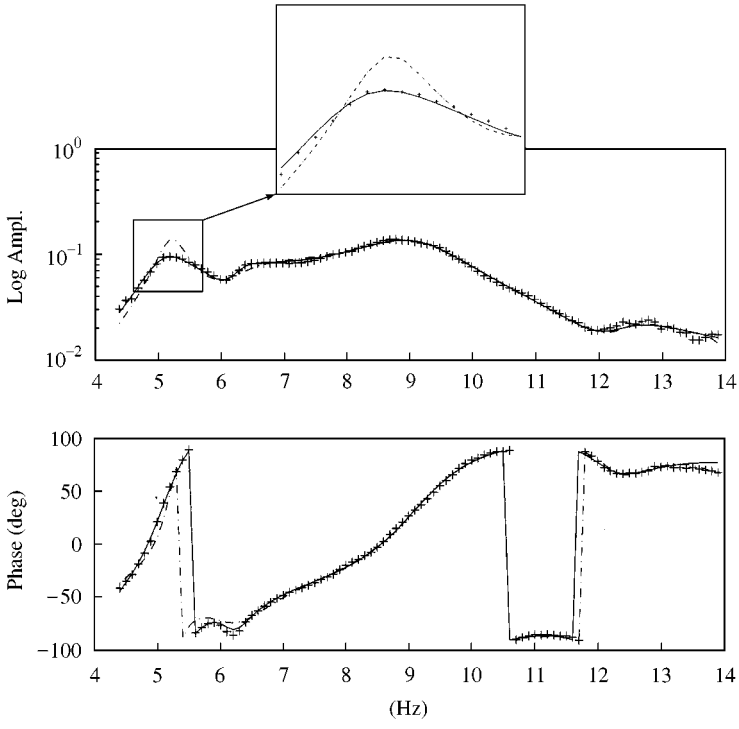


Figure 4. Transmissibility between $y_3(t)$ and $x(t)$ (+: experimental data, — GST, – · – RFP).

TABLE 1

*Modal parameters determined by GST and RFP*

| | GST | RFP |
|---|---|---|
| $f_1$ (Hz) | 5·14 | 5·22 |
| $\zeta_1$ | 8·22% | 4·16% |
| $f_2$ (Hz) | 6·27 | 6·41 |
| $\zeta_2$ | 6·07% | 12·81% |
| $f_3$ (Hz) | 9·13 | 9·17 |
| $\zeta_3$ | 9·46% | 9·46% |
| $f_4$ (Hz) | 12·29 | 12·46 |
| $\zeta_4$ | 6·08% | 4·65% |

conditions. The car-body was excited by using electrodynamic shakers at four points in correspondence with the points of attachment of the vehicle suspension systems, two positioned vertically and two horizontally in order to excite the principal global bending and torsional modes (see Figure 6). By using triaxial accelerometers positioned at 117 points distributed across the car body, a total of 1404 FRFs were measured over a range of 0–200 Hz.

The bandwidth for analysis was selected to be 15–200 Hz, which was divided into nine approximately equal sub-intervals. By applying the GST to each sub-interval a total of

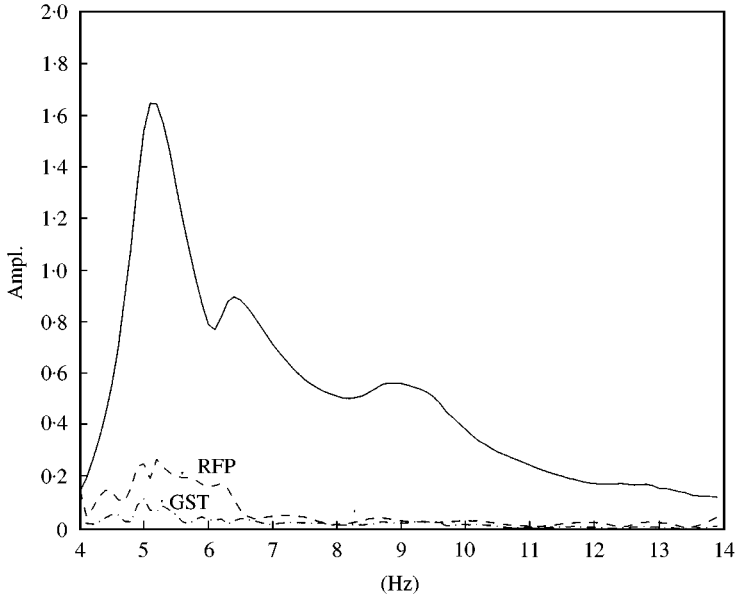


Figure 5. Cumulative transmissibility (—) and true error fitting related to GST (– · –) and to RFP (– –).

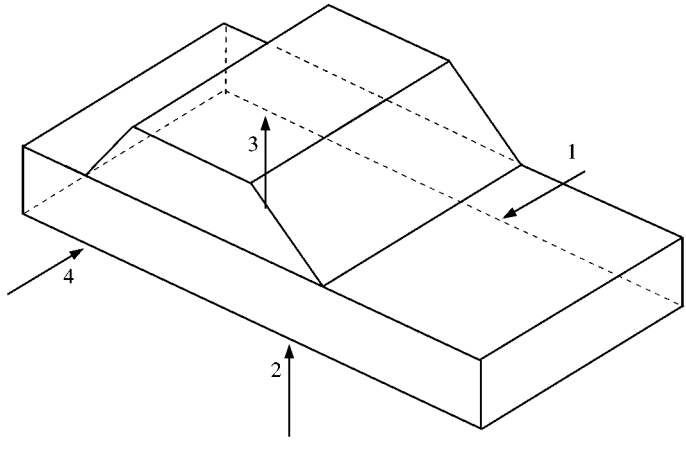


Figure 6. Shaker's locations on the car body.

39 poles were determined, so that, as the final step, it was possible to refit in the entire interval all the FRFs by using a common least-squares frequency domain (LSFD) method [14] to estimate just residues of the partial fraction description [2].

Figures 7–10 illustrate FRFs corresponding to a response point close to actuator no. 1 (called AS01) in the vertical direction and each of the four excitations respectively. As can be observed, GST provides a very accurate estimate for natural frequencies and damping ratios, with a close curve-fit being obtained by using LSFD even around the antiresonances where other techniques commonly provide poor results.

To indicate the potential of the GST with respect to other curvefitting methods, the so-called frequency domain direct parameter identification (FDDPI), available in the software package LMS-CadaX [16] and often used for examples of this type, was applied in

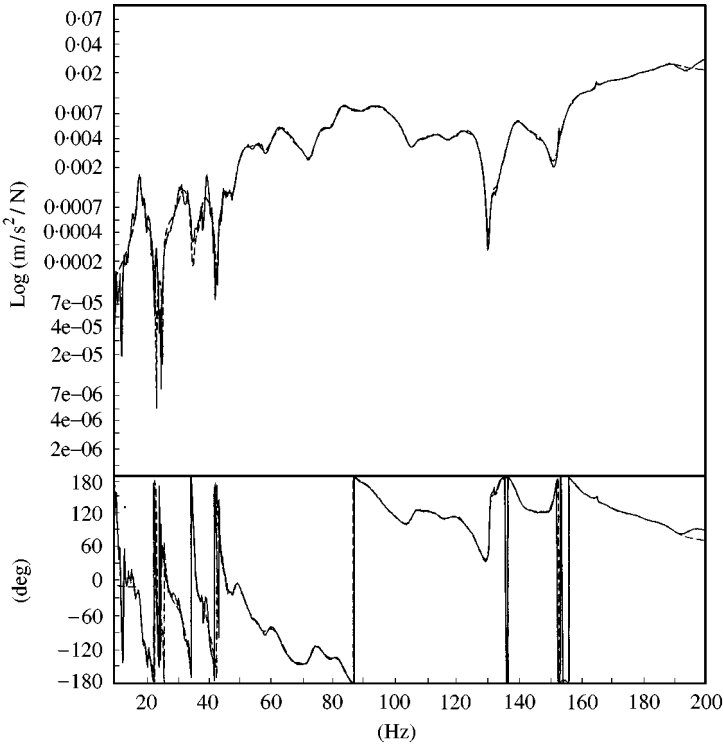


Figure 7. Fitting for FRF between point AS01 direction $Z$ and shaker no. 1, (– – GST, — experimental data).

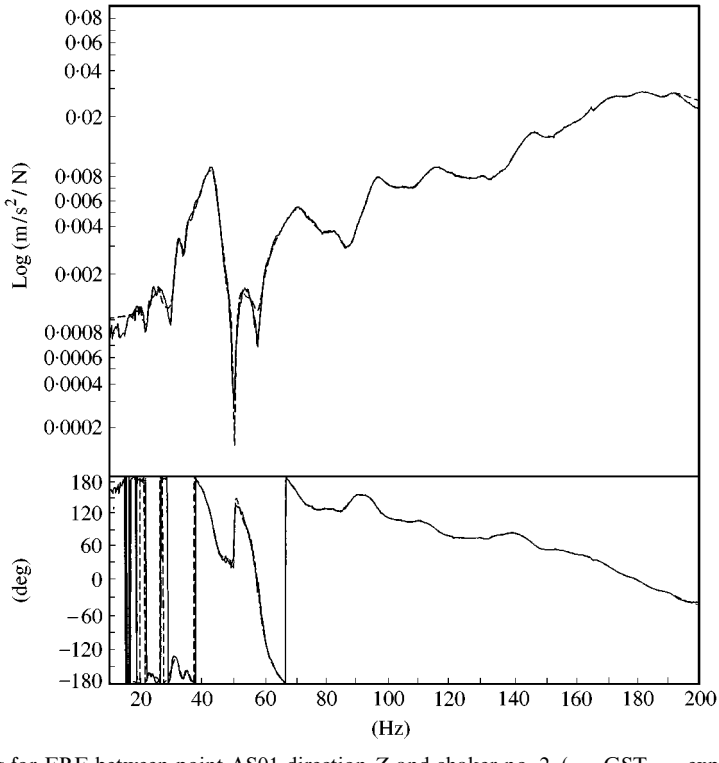


Figure 8. Fitting for FRF between point AS01 direction $Z$ and shaker no. 2, (– – GST, — experimental data).

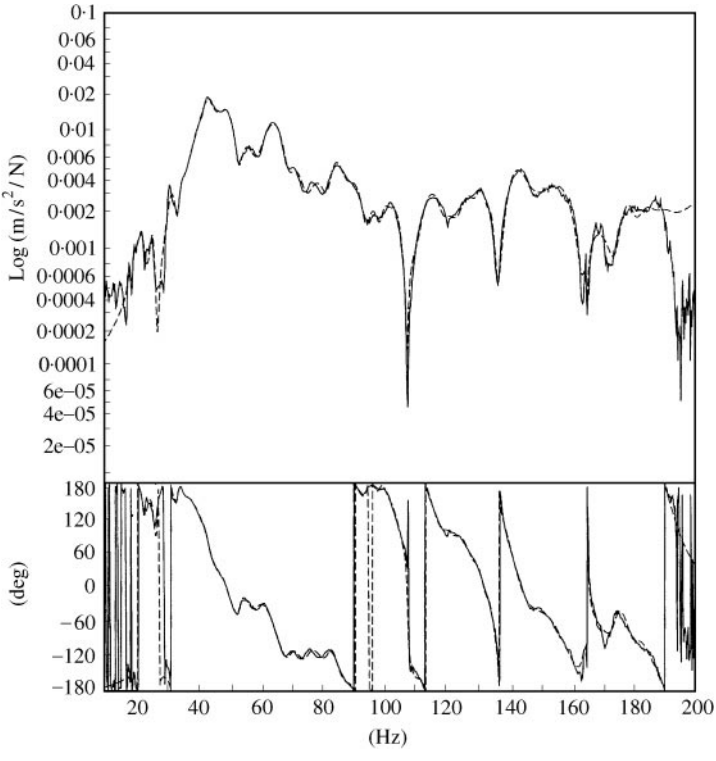


Figure 9. Fitting for FRF between point AS01 direction $Z$ and shaker no. 3, (– – GST, — experimental data).

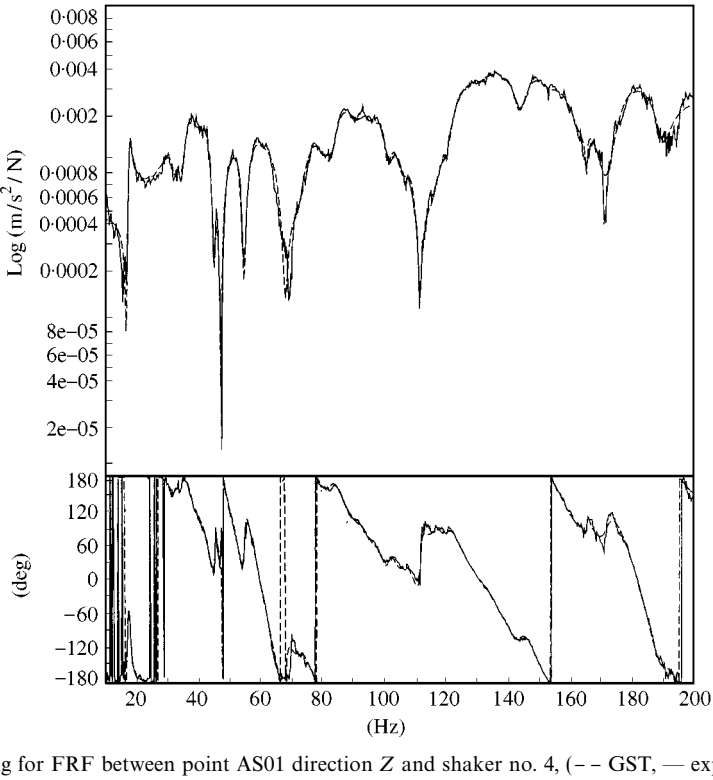


Figure 10. Fitting for FRF between point AS01 direction $Z$ and shaker no. 4, (– – GST, — experimental data).

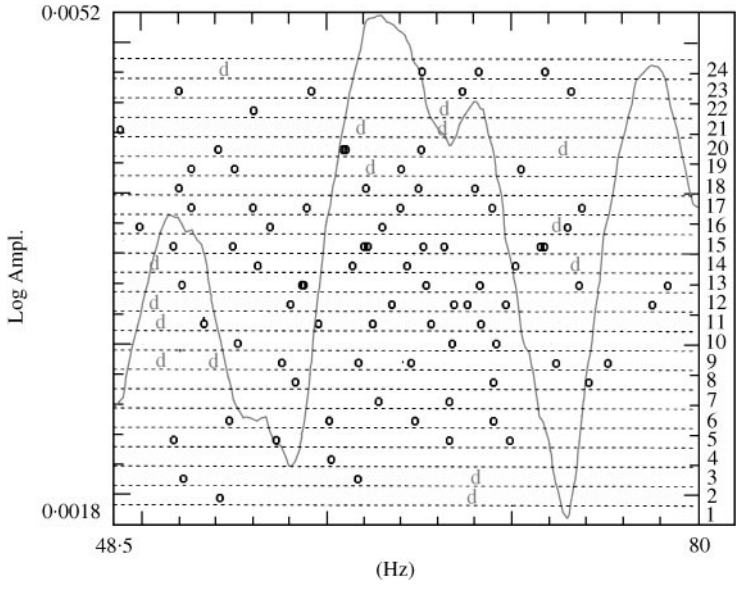


Figure 11. Stabilization diagram obtained with the FDDPI method.

the same sub-intervals chosen for GST. A typical stabilization diagram resulting from the application of this technique in the interval from 48·5 to 80 Hz is shown in Figure 11 although this does not provide any clear indication for selecting the true system poles. Whereas the GST yielded 5 poles, the FDDPI does not provide any reliable estimate for natural frequencies and damping ratios which remain stable even if the dimension of the problem to be solved is increased, a fact which serves to demonstrate the difficulty associated with conventional routines for curvefitting FRFs measured from a system with high modal coupling such as a trimmed car body.

## 4. CONCLUSIONS

This article has described a method called global smoothing technique (GST) which has been developed in order to determine the poles of structural systems for measured FRFs even when the system exhibits complex dynamic behaviour due to high modal coupling, traditionally difficult to analyze with conventional, commonly available curve-fitting routines.

Two examples of interest in the automotive industry have been studied to demonstrate the potential advantages of the GST with respect to other more conventional modal analysis methods, namely the identification of the rigid-body modes of a car engine from data measured on a road-simulated test facility, and the modal analysis of FRF data from a fully trimmed car body.

Being beyond the scope of this study, a complete comparative analysis with other more conventional modal analysis techniques will be the subject of future research. Nevertheless, the relatively high quality of the results obtained by using the GST in the case studies serves to demonstrate the potential of the method developed, particularly with regard to the more challenging and difficult-to-analyze structural systems, often relevant in different sectors of engineering.

## ACKNOWLEDGMENTS

The authors would like to thank Dr. S. Gatti for the help in applying this technique to car body data.

## REFERENCES

1. W. HEYLEN, S. LAMMENS and P. SAS 1995 *Modal Analysis Theory and Testing*. Katholieke Universiteit Leuven.
2. P. GUILLAUME, R. PINTELON and J. SCHOUKENS 1996 *Proceedings of the* 21*st International Seminar on Modal Analysis*, 1069–1082, Parametric identification of multivariable systems in the frequency domain — a survey.
3. R. DAT and J. L. MEURZEC 1972 *La Recherche Aérospatiale* **4**, 209–215. Exploitation par lissage mathématique des mesures d'admittance d'un systèm linéaire.
4. F. FERRO 1990 *Degree Thesis*, *Politecnico di Torino*. Optimization of a finite element model to correlate flight and ground vibration tests (in Italian).
5. R. RUOTOLO, W. BASSO and C. SURACE 1996 *Proceedings of Eurodyn* **96**, 1125–1132. Flight flutter test data analysis.
6. A. CARCATERRA and W. D'AMBROGIO 1995 *Meccanica* **30**, 63–75. An iterative rational fraction polynomial technique for modal identification.
7. A. CARCATERRA and A. SESTIERI 1995 *Meccanica* **30**, 77–92. Bias in modal parameters using the direct and iterative RFP identification procedure.
8. M. H. RICHARDSON and D. L. FORMENTI 1982 *Proceedings of the I International Modal Analysis Conference* 167–186. Parameter estimation from frequency response measurements using rational fraction polynomials.
9. R. RUOTOLO, D. M. STORER and L. TADDEUCCI 1997 *Proceedings of the XV International Modal Analysis Conference*. Development of a technique to determine the modal characteristics of structures using response data.
10. Matlab 1996 *The Language of Technical Computing — Using Matlab*. The Math-works Inc.
11. A. W. PHILLIPS and R. J. ALLEMANG 1996 *Proceedings of the* 21*st International Seminar on Modal Analysis*, *Leuven*, 1097–1109. Numerical considerations in modal parameter estimation.
12. G. E. FORSYTHE 1957 *SIAM Journal* **5**, 74–88. Generation and use of orthogonal polynomials for data-fitting with a digital computer.
13. H. VAN DER AUWERAER and J. LEURIDAN 1987 *Mechanical Systems and Signal Processing* **1**, 259–272. Multiple input orthogonal polynomial parameter estimation.
14. S. O' F. FAHEY and J. PRATT 1998 *Experimental Techniques* **22**, 33–37. Frequency domain modal estimation techniques.
15. J. W. DETTMAN 1969 *Mathematical Methods in Physics and Engineering*. New York: McGraw-Hill.
16. *Cada-X User Manual*. Leuven, Belgium: LMS International.